COMMUNICATION

Catalytic Hydrogenation Enabled by Ligand-Based Storage of Hydrogen

Andrew J. McNeece,[†] Kate A. Jesse,[†] Alexander S. Filatov, Joseph E. Schneider, John S. Anderson[a]

Received 00th January 20xx,
Accepted 00th January 20xx

DOI: 10.1039/x0xx00000x

Abstract Biology employs exquisite control over proton, electron, H-atom, or H_2 transfer. Similar control in synthetic systems has the potential to facilitate efficient and selective catalysis. Here we report a dihydrazonopyrrole Ni complex where an H_2 equivalent can be stored on the ligand periphery without metal-based redox changes and can be leveraged for catalytic hydrogenations. Kinetic and computational analysis suggests ligand hydrogenation proceeds by H_2 association followed by H–H scission. This complex is an unusual example where a synthetic system can mimic biology's ability to mediate H_2 transfer via secondary coordination sphere-based processes.

The controlled transfer of multiple equivalents of protons and electrons is fundamental to many important chemical reactions. While H_2 is a potent reducing agent, transition metal catalysts are often required to overcome kinetic barriers to activating H_2. Transition metals often mediate reductive transformations via hydride intermediates arising from oxidative addition of H_2 which then perform insertion reactivity.[1] While this primary sphere H_2 transfer is well-established, especially with second- or third-row metals, such two electron processes can be much more challenging with first-row metals.

One strategy to improve the reactivity of first row complexes in these transformations is to engage the secondary coordination sphere. Nature uses this approach, frequently relying on proton/electron transfer from the protein scaffold or cofactors to supply reducing equivalents to transition metal active sites.[2] The elegance of these systems has inspired synthetic chemists to discover new molecular systems which can mimic this reactivity. Incredible advances have been made in designing ancillary ligand scaffolds that can mediate electron transfer,[3] hydrogen bonding,[4] or proton shuttling.[5] Nevertheless, supporting ligand systems which can store both protons and electrons are still uncommon.[6] Recently several well-defined systems that can reversibly store H-atom equivalents have been reported.[7] Systems that can store full H_2 equivalents in a supporting ligand backbone are still rare.[8]

In order to explore this relatively scarce area we have been investigating reversible ligand-based H_2 transfer using dihydrazonopyrrole (DHP) complexes of Ni.[9] The 2,5-pyrrole pincer scaffold is attractive for this reactivity because $2e^-$ reduction/oxidation of the conjugated system coupled with protonation/deprotonation of the pincer arms can reversibly transfer H_2 without any redox changes at the metal center (Scheme 1). We have previously demonstrated that this scaffold can support the storage of both protons and electrons, but this reactivity had been limited to storage of an electron or H-atom equivalent, not storage of a full H_2 equivalent.[9a,b] We now report that Ni complexes of the previously reported $^{t\text{Bu,Tol}}$DHP ligand ($^{t\text{Bu,Tol}}$DHP = 2,5-bis((2-*t*-butylhydrazono)(*p*-tolyl)methyl)-pyrrole) can support secondary sphere storage of H_2 across the ligand backbone. Furthermore, this reactivity is reversible and enables hydrogenation catalysis. Kinetic and computational analysis indicates that ligand hydrogenation proceeds in a process that is first-order in [Ni] and involves H_2 association followed by H–H scission.

Deprotonation of the previously reported $^{t\text{Bu,Tol}}$DHP•2HCl with 3 eq. of *n*-BuLi followed by dropwise addition to (dme)$NiCl_2$ (dme = 1,2-dimethoxyethane) in THF provides ($^{t\text{Bu,Tol}}$DHPH_2)NiCl (**1**) as a red crystalline solid in 56% yield (Scheme 2). The ^{1}H NMR spectrum of **1** shows diamagnetic signals indicating a symmetric DHP environment, with a new broad singlet resonance at 5.98 ppm which is assigned to the two N–H protons on the ligand scaffold (see ESI). Analysis by single crystal X-ray diffraction (SXRD) shows a twisted square-planar complex

Scheme 1. Ligand based storage of H_2 on dihydrazonopyrrole scaffolds.

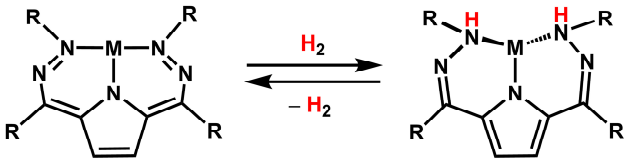

[a] *University of Chicago Department of Chemistry, 929 E 57th St. Chicago, IL, 60637*
Electronic Supplementary Information (ESI) available: [details of any supplementary information available should be included here]. See DOI: 10.1039/x0xx00000x
[†] These authors contributed equally

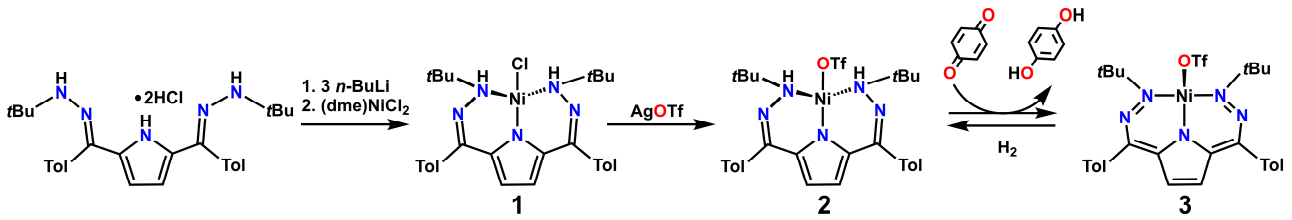

Scheme 2. Synthesis of **1** and **2** and interconversion of **2** and **3** with H_2 and benzoquinone.

with the Ni square plane rotated from the plane of the central pyrrole ring by ~30° (Figure 1, top). The Ni–$N_{hydrazone}$ bonds are 1.938(2) and 1.946(2) Å, which are ~0.1 Å longer than those seen in the previously reported T-shaped complex (^{tBu,Tol}DHP$^{\bullet}$)Ni, likely due to both weaker donation and greater steric strain from the protonated nitrogens. Within the ligand scaffold, the N–N bonds are 1.454(3) and 1.460(2) Å which are significantly longer than other ^{tBu,Tol}DHP or ^{Ph,Tol}DHP complexes (~1.37 Å), supporting ligand-based redox changes. The N–H protons can be located in the difference map, and are oriented towards the Cl ligand. The Cl···H distances are ~2.55 Å and the N–H–Cl angles are 104°. Both of these values are consistent with hydrogen bonding interactions, as have been observed in other M–Cl complexes.[10] Distinct stretches are also observed by IR spectroscopy at 3241 and 3166 cm^{-1}, further confirming the presence of N–H groups (see ESI).

We then investigated the reactivity of **1** to determine whether the ligand-stored H_2 equivalent could be transferred to substrates. However, **1** shows little to no reactivity with substrates including air, olefins, and carbonyls. We hypothesized that a comparatively strongly coordinating Cl^- ligand might inhibit reactivity by occupying a potential site of substrate coordination and therefore abstracted this ligand. Complex **1** reacts cleanly with AgOTf to give the corresponding triflate complex (^{tBu,Tol}DHPH$_2$)NiOTf (**2**) (Scheme 1). SXRD analysis shows a structure very similar to that of **1** with the triflate bound in the fourth coordination site (Figure 1, bottom). Hydrogen bonding interactions to the triflate ligand are also clear, with one interaction to O2 of moderate strength and two weaker interactions to O1 based on O···H distances of ~1.9 and 2.4 Å respectively.

We then turned to see if this ligand substitution enabled H_2 transfer reactivity. Hydrogen transfer was tested by stirring **2** with benzoquinone at room temperature which resulted in slow formation of hydroquinone and the previously reported dehydrogenated complex (^{tBu,Tol}DHP)NiOTf (**3**) as indicated by ^{1}H NMR spectroscopy (Scheme 1, see ESI).[9c] This reactivity demonstrates an unusual example where an H_2 equivalent stored on a ligand backbone can be transferred to a substrate. Examples of H_2 transfer between a supporting ligand and a substrate are rare.[8]

In order to determine whether catalytic H_2 transfer was possible, we then investigated whether **2** could be regenerated from **3** with H_2 gas. Encouragingly, ^{1}H NMR analysis of this reaction indicates that complex **2** is formed as the major product when **3** is reacted with one atmosphere of H_2 with mild heating (see ESI). Given this result, we then placed **3** and excess benzoquinone under an atmosphere of H_2 to determine whether catalytic hydrogenation was feasible. Monitoring by ^{1}H NMR spectroscopy at room temperature shows conversion of **3** to **2** with concomitant conversion of two equivalents of benzoquinone to hydroquinone indicating this process is catalytic (see ESI). This reactivity provides important proof of concept for ligand-based H_2 transfer and shows the viability of the DHP scaffold for reversible H_2 donation.

We were interested in understanding more about the mechanistic details of addition of H_2 to the ligand backbone and therefore we performed kinetic analyses on the interconversion of **3** and **2**. Monitoring the reaction of **3** with H_2 by UV-visible

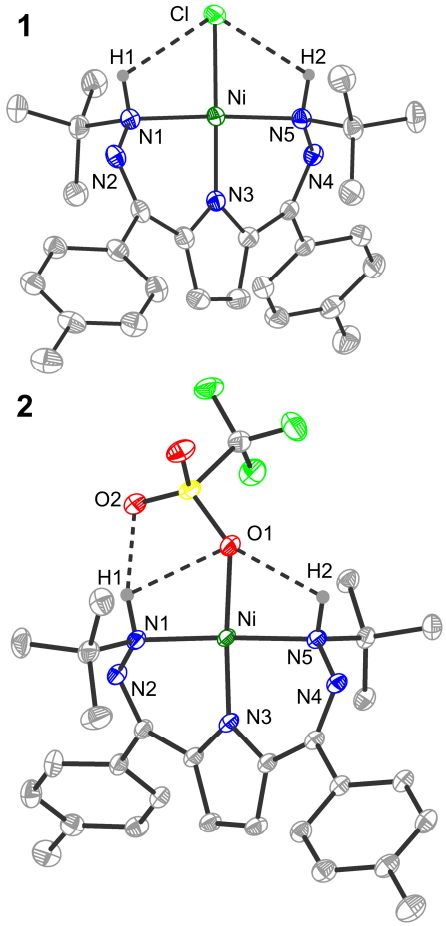

Figure 1. Solid state structure of **1** (top), and **2** (bottom) with ellipsoids set to 50% probability, and all C–H hydrogens omitted for clarity. Hydrogen bonding interactions shown with dashed lines. Ni shown in green, C in grey, N in blue, O in red, F in bright green, Cl also in bright green (labelled), and S in yellow. Selected bond lengths (Å): **1**: Ni–Cl: 2.1817(7) Å, Ni–N1: 1.938(2), Ni–N3: 1.824(2), Ni–N5: 1.946(2), N1–N2: 1.454(3), N4–N5: 1.460(2). **2**: Ni–O: 1.952(1) Å, Ni–N1: 1.955(1), Ni–N3: 1.812(1), Ni–N5: 1.964(1), N1–N2: 1.455(2), N4–N5: 1.460(2).

spectroscopy shows conversion of **3** to **2** with kinetics consistent with a first-order reaction in [Ni] under pseudo first-order conditions (Figure 2). Comparison of the product peak intensities at 355 nm with intensities from isolated **2** indicates a high yield for this conversion (>80%), consistent with ^{1}H NMR analysis (see ESI), but some small amount of an intermediate or byproduct with an absorbance around 550 nm is also formed. We have thus far been unable to obtain further information on this species. The first order dependence on [Ni] for the consumption of **3** is consistent with the hypothesis of a single metal complex reacting to store H_2 across the ligand framework as opposed to a bimolecular reaction, as has been observed in the homolytic activation of O–H bonds with a related ^{Ph,Tol}DHP complex.[9b]

An Eyring analysis shows a $\Delta H^{\ddagger}$ of 13.9(4) kcal/mol and $\Delta S^{\ddagger}$ of −18(5) cal/(molK), which gives an overall $\Delta G^{\ddagger}$ at 298 K of ~21 kcal/mol (Figure 2). The comparatively large and negative $\Delta S^{\ddagger}$ suggests that association of H_2 is at least rate-contributing. We also performed the same analysis with D_2 to determine the deuterium kinetic isotope effect (KIE) for this hydrogenation reaction. Comparison of the rates under H_2 versus D_2 shows an inverse deuterium KIE of 0.8(1). If scission of the H–H bond was the sole rate contributing step a normal primary KIE would be expected. In contrast, the observed inverse KIE for this hydrogenation reaction could potentially arise from an equilibrium isotope effect (EIE) in an H_2 binding pre-equilibrium.[11] For this reason, as well as the convolution of the energetics of the H_2 cleavage steps by an H_2 association step, we have examined this reaction in more detail through additional calculations.

We have examined the thermodynamics of H_2 addition to the ligand framework by performing density functional theory (DFT) calculations. We initially attempted calculations on OTf^{-}-bound species but observed dissociation of the anion along the reaction coordinate. Experimental evidence for OTf– dissociation is equivocal (see ESI), but the increased reactivity on moving from **1** to **2** supports that anion dissociation may be required for reactivity. To simplify our computational analysis, we have instead examined the energetics and geometries of H_2 cleavage along a singlet manifold starting from a putative cationic intermediate $[(^{tBu,Tol}DHP)Ni]^{+}$ (Figure 3).

The first optimized transition state is an H_2 splitting step across the Ni–N bond to form the intermediate hydride species $[(^{tBu,Tol}DHPH)NiH]^{+}$. This transition state is 28.4 kcal/mol higher in energy than $[(^{tBu,Tol}DHP)Ni]^{+} + H_2$. The second transition state has a similar barrier of 25.9 kcal/mol versus $[(^{tBu,Tol}DHP)Ni]^{+} + H_2$ and results in the favorable (–6.5 kcal/mol from the reactants) formation of the hydrogenated product. Examining the Mulliken charge densities of the H-atoms along the reaction coordinate suggests that TS1 is best described as a proton transfer (see ESI). While the charges in TS2 are much more covalent, the balanced reaction and Mulliken charges suggests this is step is best considered as a hydride transfer. Overall, this analysis suggests that H_2 binding and scission should be accessible with reasonably good agreement between theoretical and experimental energetics.

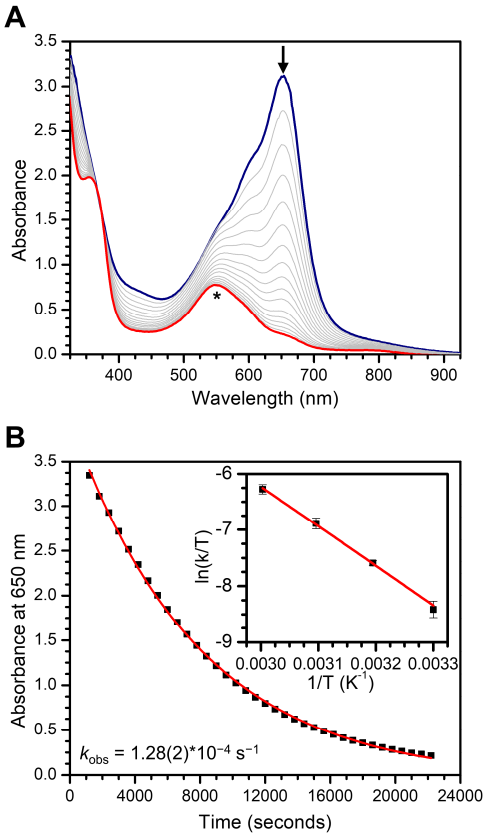

Figure 2. Kinetic analysis of the hydrogenation of **3** to **2**. (A) UV-vis traces of **3** under 1 atmosphere of H_2 at 40 °C taken every 10 minutes. The asterisk indicates a small but intensely colored impurity. (B) Decay of the absorbance at 650 nm with an exponential fit as described in the ESI shown in red. Inset: Eyring analysis with linear fit (R^2 = 0.99) in red to determine the activation parameters for the hydrogenation as described in the text and ESI.

These calculations also enable us to test the origin of the inverse experimental KIE. Examination of the isotope dependence of the first transition state (TS1) suggests that a primary KIE would be expected (see ESI), in contrast with experimental observations. Conversely, if the isotope dependence of free H_2/D_2 and $LNiH_2^{+}/LNiD_2^{+}$ are considered, an inverse isotope dependence is predicted for reversible H_2 binding, consistent with experiment (see ESI). These observations suggest that the origin of the observed isotope dependence likely arises from an H_2 association EIE.[11] Similar inverse isotope effects have recently been observed in paramagnetic transition metal systems as well as across bimetallic frustrated Lewis pairs.[12,13]

The studies presented here show an unusual example of metal-ligand cooperativity enabled hydrogenation reactivity where the ligand can store a full H_2 equivalent. The catalytic hydrogenation of benzoquinone provides an important proof of concept for this area. Kinetic data show that the bifunctional splitting of H_2 proceeds in a process that is first-order in [Ni], but that proceeds with an inverse deuterium isotope dependence. Calculations suggest that H_2 scission is energetically accessible and that the source of the observed inverse deuterium isotope dependence is an EIE arising from H_2 association. While catalytic hydrogenations of other substrates have been less successful

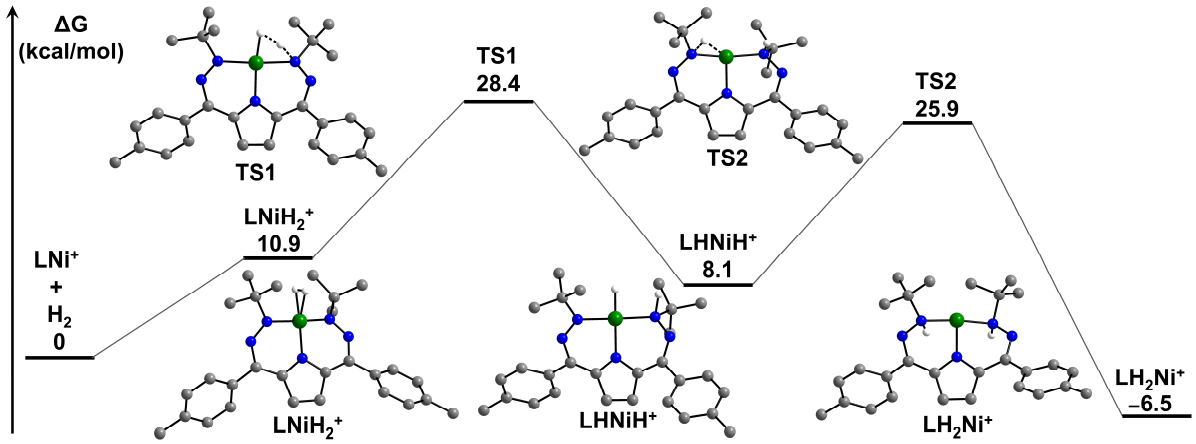

Figure 3. DFT computed geometries and energies of H_2 splitting. Calculations were carried out with the B3P functional and a def2-TZVP basis set, with a def2-TZVPP basis set on Ni. Ni is shown in green, C in gray, N in blue, and H in white. Note that only H-atoms stemming from the H_2 ligand are shown.

thus far, the enhanced reactivity in moving from **1** to **2** (Cl^- to OTf^-) suggests that the primary metal coordination sphere still plays an important role in this primarily ligand-centered reactivity and offers a potential avenue to expand hydrogenation reactivity to other substrates.

This work was supported by the National Institutes of Health (R35 GM133470). We thank the University of Chicago for funding, the 3M Corporation for a NTFA to J.S.A., and the Sloan Foundation for a Research Fellowship to J.S.A. (FG-2019-11497). J.E.S. was supported by the Department of Defence through a National Defence Science and Engineering Graduate fellowship (00003765). We also thank the Research Computing Center at the University of Chicago for providing computing resources. We would like to than Dr. Josh Kurutz for assistance with NMR. Some data reported here were collected at ChemMatCARS Sector 15 which is supported by the NSF under grant number NSF/CHE-1834750. This research used resources of the APS, a U.S. DOE Office of Science User Facility operated for the DOE Office of Science by Argonne National Laboratory under Contract No. DE-AC02-06CH11357. We would like to thank Dr. Yu-Sheng Chen and Dr. SuYin Wang for assistance with SXRD acquisition at 15-ID-B,C,D.

Conflicts of interest

There are no conflicts to declare.

Notes and references

†These authors contributed equally.

[1] R. H. Crabtree, *Organometallic Chemistry of the Transition Metals, 6th Edition*, 2014.

[2] (a) S. A. Cook, E. A. Hill and A. S. Borovik, *Biochemistry*, 2015, **54**, 4167-4180. (b) D. F. Baumgardner, W. E. Parks and J. D. Gilbertson, *Dalton Trans.*, 2020, **49**, 960-965.

[3] (a) O. R. Luca and R. H. Crabtree, *Chem. Soc. Rev.*, 2013, **42**, 1440-1459. (b) R. Arevalo and P. J. Chirik, *J. Am. Chem. Soc.*, 2019, **141**, 9106-9123.

[4] S. A. Cook and A. S. Borovik, *Acc. Chem. Res.*, 2015, **48**, 2407-2414.

[5] (a) M. Rakowski Dubois and D. L. Dubois, *Acc. Chem. Res.*, 2009, **42**, 1974-1982. (b) T. Zell and D. Milstein, *Acc. Chem. Res.*, 2015, **48**, 1979-1994. (c) M. L. Pegis, C. F. Wise, D. J. Martin and J. M. Mayer, *Chem. Rev.*, 2018, **118**, 2340-2391.

[6] L. Alig, M. Fritz and S. Schneider, *Chem. Rev.*, 2019, **119**, 2681-2751.

[7] (a) E. J. Thompson and L. A. Berben, *Angew. Chem. Int. Ed.*, 2015, **54**, 11642-11646. (b) G. W. Margulieux, M. J. Bezdek, Z. R. Turner and P. J. Chirik, *J. Am. Chem. Soc.*, 2017, **139**, 6110-6113. (c) A. Dauth, U. Gellrich, Y. Diskin-Posner, Y. Ben-David and D. Milstein, *J. Am. Chem. Soc.*, 2017, **139**, 2799-2807. (d) K. E. Rosenkoetter, M. K. Wojnar, B. J. Charette, J. W. Ziller and A. F. Heyduk, *Inorg. Chem.*, 2018, **57**, 9728-9737. (e) M. B. Ward, A. Scheitler, M. Yu, L. Senft, A. S. Zillmann, J. D. Gorden, D. D. Schwartz, I. Ivanović-Burmazović and C. R. Goldsmith, *Nature Chem.*, 2018, **10**, 1207-1212. (f) M. J. Drummond, C. L. Ford, D. L. Gray, C. V. Popescu and A. R. Fout, *J. Am. Chem. Soc.*, 2019, **141**, 6639-6650.

[8] (a) B. W. Purse, L. H. Tran, J. Piera, B. Åkermark and J. E. Bäckvall, *Chem. Eur. J.*, 2008, **14**, 7500–7503. (b) T. W. Myers, L. A. Berben, *Chem. Sci,.* 2014**, 5**, 2771-2777 (c) J. T. Henthorn, S. Lin and T. Agapie, *J. Am. Chem. Soc.*, 2015, **137**, 1458-1464. (d) P. O. Lagaditis, B. Schluschaß, S. Demeshko, C. Würtele and S. Schneider, *Inorg. Chem.*, 2016, **55**, 4529-4536. (e) F. Schneck, M. Finger, M. Tromp and S. Schneider, *Chem. Eur. J.*, 2017, **23**, 33-37. (f) B. M. Lindley, Q. J. Bruch, P. S. White, F. Hasanayn and A. J. M. Miller, *J. Am. Chem. Soc.*, 2017, **139**, 5305–5308. (g) R. Pramanick, R. Bhattacharjee, D. Sengupta, A. Datta and S. Goswami, *Inorg. Chem.*, 2018, **57**, 6816-6824. (h) R. Jain, A. A. Mamun, R. M. Buchanan, P. M. Kozlowski and C. A. Grapperhaus, *Inorg. Chem.*, 2018, **57**, 13486-13493. (i) T. J. Sherbow, E. J. Thompson, A. Arnold, R. I. Sayler, R. D. Britt, L. A. Berben, *Chem. - Eur. J.,* 2019, **25**, 454-458.

[9] (a) M-C. Chang, A. J. McNeece, E. A. Hill, A. S. Filatov, J. S. Anderson. *Chem. Eur. J.*, 2018, **24**, 8001-8008. (b) M-C. Chang, K. A. Jesse, A. S. Filatov, J. S. Anderson, *Chem Sci.*, 2019, **10**, 1360-1367. (c) A. J. McNeece, K. A. Jesse, J. Xie, A. S. Filatov, J. S. Anderson, *J. Am. Chem. Soc.* 2020, **142,** 10824-10832.

[10] (a) G. Aullón, D. Bellamy, A. Guy Orpen, L. Brammer and Eric A. Bruton, *Chem. Commun.*, 1998, 653-654. (b) T. Steiner, *Angew. Chem. Int. Ed.*, 2002, **41**, 48-76.

[11] (a) W. D. Jones, *Acc. Chem. Res.*, 2003, **36**, 140-146. (b) D. G. Churchill, K. E. Janak, J. S. Wittenberg and G. Parkin, *J. Am. Chem. Soc.*, 2003, **125**, 1403-1420. (c) M. Gómez-Gallego and M. A. Sierra, *Chem. Rev.*, 2011, **111**, 4857-4963. (d)

[12] Y. Zhang, M. K. Karunananda, H.-C. Yu, K. J. Clark, W. Williams, N. P. Mankad and D. H. Ess, *ACS Catalysis*, 2019, **9**, 2657-2663.

[13] D. E. Prokopchuk, G. M. Chambers, E. D. Walter, M. T. Mock and R. M. Bullock, *J. Am. Chem. Soc.*, 2019, **141**, 1871-1876.